Surface-Enhanced Raman Spectra of Phthalimide. Interpretation of the SERS Spectra of the Surface Complex Formed on Silver Islands and Colloids

R. F. Aroca* and R. E. Clavijo†

Materials and Surface Science Group, School of Physical Sciences, University of Windsor, Windsor, Ontario, Canada N9E 3P4

M. D. Halls and H. B. Schlegel

Department of Chemistry, Wayne State University, Detroit, Michigan 48202

Received: June 8, 2000; In Final Form: July 31, 2000

The surface-enhanced Raman scattering (SERS) spectra for phthalimide (PIMH) vacuum evaporated, cast onto silver island films, and from colloidal silver are clearly identified with the formation of a phthalimide−silver complex (chemisorption). The phthalimide−silver complex (PIMAg) has been obtained from the PIMH potassium salt and $AgNO_3$. The Raman scattering spectrum of the isolated complex is in agreement with the SERS spectra of the silver surface complex. The experiments were carried out using three laser lines at 514.5, 633, and 780 nm. The photochemical decomposition of the surface complex is detected with all laser lines. The spectral interpretation is aided using Hartree−Fock and local density functional theory (S-VWN) calculations, carried out to compute simulated SERS spectra using the molecular complex PIMAg and the PIMH. The calculated surface complex (SERS) Raman spectrum using S-VWN was found to be in good agreement with the observed spectrum. The observed Raman spectrum for the surface complex may contain the Raman-active modes allowed in the total irreducible representation of the complex symmetry point group. However, the number of observed vibrations can be reduced due to further constraints introduced by molecular and field orientations at the surface (surface selection rules or propensity rules).

Introduction

Following its initial observation by Fleischman et al.,[1] and subsequent identification,[2,3] surface-enhanced Raman scattering (SERS) has revolutionized the vibrational spectroscopy at surfaces and interfaces. With the advent of surface-enhanced infrared spectroscopy, a new branch of vibrational spectroscopy, the surface-enhanced vibrational spectroscopy (SEVS), has been established.[4] However, the development of SERS into a widespread analytical tool has been hampered by the fact that specially prepared rough surfaces are required and that the interpretation of the SERS spectrum poses a challenge for most adsorbates. At the same time, the most recent achievement of SERS has been to bring vibrational spectroscopy into the ranks of single molecule spectroscopies, with reports that the enhanced Raman cross sections would allow the detection of single molecules using the technique.[5,6]

The origin of the enhancement of Raman scattering cross sections at rough metal surfaces has been an active field of research. The general consensus attributes the observed enhancement to contributions from two mechanisms: an electromagnetic enhancement and a chemical effect.[7,8] Notably, both mechanisms were suggested in the original interpretation papers.[2,3] Jeanmaire and Van Duyne's initial discussion contains the first theoretical model to interpret the origin of the enhanced signal: "The postulation of an electric field enhancement permits further comment on the surface orientation and the Raman signal strength". The latter statement is followed by an example of the additional constraints imposed on the allowed Raman vibrational frequencies of the free molecule, by the molecular orientation at the surface, and the electric field polarization at the metal surface. These constrains will be later introduced as surface selection rules or propensity rules. On the other hand, the most challenging case arises when the molecule is chemically adsorbed onto the rough surface. A surface complex is formed with new electronic states that could be in-resonance with the exciting laser line given rise to resonant Raman scattering (RRS) as pointed out by Albrecht and Creighton.[3] Depending on the SERS-active substrate used and the nature of the molecular system to be studied, each of the two SERS enhancement mechanisms can have dramatically different significance. For physisorbed randomly oriented molecules, where electromagnetic enhancement (EM) is the dominant mechanism, the interpretation of the SERS spectra based on the SERS EM theory is, in most cases, straightforward, provided the reference molecule Raman spectra is available. When the molecules are chemically adsorbed to the surface, the interpretation of the observed SERS spectra is more challenging. Bonding to the surface perturbs the electronic structure of the adsorbate and the formation of the surface complex causes significant deviation from the reference Raman spectrum; therefore, it of interest to examine the SERS spectra in the case of chemisorption. Chemisorption can be defined as adsorption with interaction energy comparable to chemical bond energies, i.e., formation of a surface complex. The present report is part of our studies on the interpretation of SERS spectra of chemisorbed species on silver island films and metal colloids. For both substrates there is an enhancement due to the EM mechanism and its

* Corresponding author. E-mail: G57@uwindsor.ca.
† Present address: Department of Chemistry, Faculty of Science, University of Chile.

10.1021/jp002071q CCC: $19.00
Published on Web 09/29/2000

properties are well-known.[8] For SERS of chemisorbed species, there are two distinct cases to consider. They correspond to the formation of a surface complex with or without electronic states that can serve as intermediates in resonance Raman scattering (RRS). A case of a surface complex given resonant Raman scattering has been recently reported.[9] Here, the results obtained for phthalimide (PIMH), an aromatic nitrogen-containing molecule that forms a surface complex on silver that gives no evidence of resonance Raman scattering in the 514.5−780 nm spectral region, are presented. The Raman spectra of PIMH have been reported previously[10,11] and complete vibrational assignments have been proposed on the basis of isotope substitution and semiempirical molecular orbital calculations.[12] The SERS spectrum of PIMH has been reported on two different SERS substrates: colloidal silver[13] and silver island films.[14] However, the SERS spectra previously reported on silver island films[14] appear completely different from those obtained for PIMH on colloidal silver.[13] Since the interpretation of the SERS spectra was not the main purpose of the report, the authors did not note the substantial difference, as they were not aware of the colloidal SERS study reported earlier. The bonding of PIMH to the surface of silver colloids[13] was supported by comparison with the SERS obtained on silver colloid for the phthalimide potassium salt and by the appearance of a characteristic N−Ag band.

In summary, the observed SERS spectra of the surface complex (chemisorption) should be completely determined by fundamental vibrational modes of the complex and the constraints imposed by the molecular orientation and electric field polarization at the surface. Interpretation of the experimental data is facilitated by progress in the efficiency of programs for computing derivative properties, such as normal-mode frequencies and spectral intensities, and advances in computer hardware that have made quantum chemical calculations an invaluable aid to spectroscopists in the analysis and assignment of experimental vibrational spectra for complex polyatomics. Density functional theory (DFT) in recent years has proved to be superior compared to conventional ab initio methods in computing quantitative vibrational properties in a cost-effective fashion. Work by Scott and Radom[15] and Wong[16] has shown that DFT predicts harmonic frequencies in excellent agreement with observed fundamentals, having empirical scaling factors close to unity.[17] Studies of the vibrational intensities furnished by DFT methods[18,19] lend additional support for the application of DFT in computing reliable theoretical vibrational spectra to assist the interpretation of spectra for unique and complex molecular systems.

The introduction of simple computational models and their validation using archetypal chemisorbed analytes is shown to be of great utility. The use of quantum chemical calculations to model SERS spectra has been reported. Schatz and coworkers have previously used Hartree−Fock and semiempirical methods to model SERS spectra and concluded that "in order to improve on the SERS predictions, it will be necessary to include for the influence of interaction between the molecule and metal".[20,21]

Experimental Section

The Raman spectra were recorded with a Renishaw system 2000 equipped with three lasers of which the 514.5, 633, and 780 nm laser lines were used to record the SERS spectra. The power at the sample location was varied from 40 μW to a maximum of 2 mW. Silver island films were prepared of 6 and 10 nm mass thickness in a Balzers vacuum system evaporator using a Balzers BSV 080 glow discharge evaporation unit. The silver island films were deposited onto a preheated glass substrate (200 °C). Ultrathin phthalimide films were then deposited onto the silver island films after cooling to room temperature. Organic films were approximately of 10, 20, and 30 nm mass thickness. During thin film deposition the background pressure was nominally 10^{-6} Torr and the deposition rate was monitored using an XTC Inficon quartz crystal oscillator. The PIMAg complex was obtained as a white precipitate by adding a $AgNO_3$ solution to an aqueous solution of phthalimide potassium salt (PIMK) of the same concentration. The precipitate was washed with deionized double-distilled water and dried at low vacuum. The Raman spectra of the light-sensitive complex were recorded using 40 μW of the 633 nm laser line. Solutions of phthalimide in acetone and ethanol were also used to spray a silver film and tested for SERS.

The theoretical calculations were carried out using the Gaussian suite of programs.[22] Hartree−Fock and DFT calculations were performed using the Lanl2DZ basis set corresponding to the D95 basis on first row atoms[23] and the Los Alamos ECP plus DZ on silver.[24] The local density functional employed in this work consisted of the Slater−Dirac exchange functional[25] with the Volsko−Wilk−Nusair fit for the correlation functional,[26] denoted S-VWN. Following geometry optimizations, harmonic frequencies and dipole moment derivatives were computed analytically. Polarizability derivatives were computed using numerical differentiation of the analytic dipole derivatives with respect to the applied electric field for S-VWN and were computed analytically for Hartree−Fock. Static Raman intensities (zero frequency, nonresonant) were computed in the double harmonic approximation,[27] ignoring cubic and higher force constants and omitting second and higher polarizability derivatives. Computed harmonic frequencies typically overestimate vibrational fundamentals due to basis set truncation and neglect of electron correlation and mechanical anharmonicity.[28] To compensate for these shortcomings, various scaling strategies exist for bringing the computed frequencies into greater coincidence with observed wavenumbers.[29−32] In this report we have employed the simplest scheme, that of homogeneous scaling. The Hartree−Fock and S-VWN frequencies were scaled using the empirical scaling factors, 0.8953 and 0.9833 respectively, as suggested by Scott and Radom, and Wong.[15,16]

Results and Discussion

Observed PIMH and PIMAg Raman Spectra. PIMH is a planar molecule with C_{2v} symmetry that has 42 normal modes of vibration, composed of 15 of a_1 symmetry (transforming as $\mathbf{x^2}$, $\mathbf{y^2}$, $\mathbf{z^2}$), 6 of a_2 symmetry (transforming as **xy**), 7 of b_1 symmetry (transforming as **xz**), and 14 of b_2 symmetry (transforming as **yz**), choosing the *x* axis to be perpendicular to the molecular plane. Therefore, all of the fundamental vibrations are Raman active and as many as 37 fundamentals could be observed in the low-frequency region of the spectrum (4 C−H stretches and 1 N−H stretch appear above 3000 cm^{-1}). Using the PIMAg as starting material, the PIMH was recovered by precipitating the Ag as AgCl. Crystals of PIMH were recovered from the dissociation of the PIMAg complex when the solvent was evaporated. The Raman spectra collected from PIMH recovered from the PIMAg salt are shown in Figure 1. The calculated Raman spectrum is also shown for comparison. The PIMH vibrational modes are well-known[10−13] and the spectrum shown in Figure 1 is in full agreement with the literature spectrum. The theoretical Raman spectrum provides a good guide to Raman intensities with the caveat that the computed

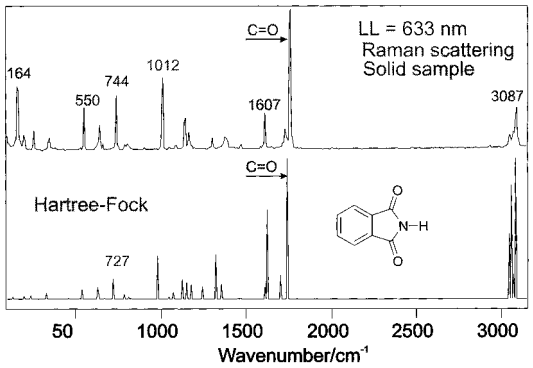

Figure 1. Raman scattering of solid phthalimide (PIMH) and calculated Hartree−Fock Raman intensities.

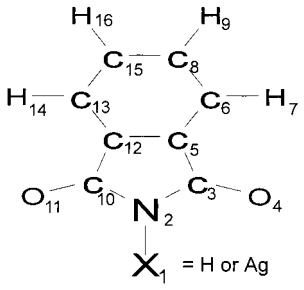

Figure 2. Molecular structure of PIMX (X = H or Ag).

spectrum is for the gas phase system. The observed relative intensities in the Raman scattering (RS) spectrum of the solid may differ significantly from the gas-phase intensities.

Raman Spectrum of the PIMAg Salt. The molecular structure of PIMAg complex is shown in Figure 2. The PIMAg salt corresponds to the parent molecule PIMH with the hydrogen replaced by an Ag atom. It therefore has the same connectivity and symmetry as the free molecule and has 42 normal modes with the total irreducible representation: $\tilde{A} = 15a_1 + 6a_2 + 7b_1 + 14b_2$. The optimized bond lengths, interatomic angles, and the change upon bonding to silver, at Hartree−Fock and S-VWN levels of theory are presented in Table 1. The geometric perturbation caused by replacing the imide hydrogen by the silver atom is localized in the five-member ring and carbonyls closest to the silver, and is negligible on the opposite side of the molecule. These geometric changes are indicative of changes in bonding upon substitution of hydrogen with silver.

The Raman scattering spectra of PIMAg excited with the 633 and 780 nm laser lines are shown in Figure 3. The scaled theoretical gas-phase Raman spectrum for PIMAg is also included in Figure 3. The RS spectrum of the PIMAg is substantially different from that of PIMH shown in Figure 1. It is also quite different from the RS spectrum of potassium salt.[13] In the Raman spectra of PIMH and PIMK the most intense band corresponds to the stretching vibration of the carbonyl groups at 1757 and 1706 cm^{-1}, respectively. The corresponding band in the RS spectrum of PIMAg is only of middle intensity. Notably, the lowering in the Raman intensity for the C═O stretching mode in PIMAg is also reproduced in the calculated HF and DFT Raman spectra. The wavenumbers of the C═O stretching mode are observed at 1706 cm^{-1} in PIMAg and PIMK, but is 1757 cm^{-1} in PIMH. The ionic character of the salts is reflected in lowering of the intensity and wavenumber of the C═O stretching mode. Comparing the theoretical spectra to the PIMAg spectra below 1100 wavenumber shows that both Hartree−Fock and S-VWN predict the same number of bands of substantial intensity. For this region, the overall agreement

TABLE 1: Geometric Parameters and the Change Therein Upom Binding to Ag at Hartree−Fock and S-VWN Levels of Theory

	Hartree−Fock			S-VWN		
	PIMH	PIM-Ag	diff	PIMH	PIM-Ag	diff
			Bond Lengths (Å)			
X_1-N_2	0.995	2.167	−1.172	1.023	2.008	−0.985
N_2-C_3	1.396	1.381	0.015	1.406	1.397	0.009
C_3-O_4	1.216	1.230	−0.014	1.242	1.249	−0.007
C_3-C_5	1.490	1.502	−0.012	1.484	1.491	−0.007
C_5-C_{12}	1.394	1.392	0.002	1.404	1.404	0.000
C_5-C_6	1.381	1.381	0.000	1.391	1.390	0.001
C_6-H_7	1.071	1.072	−0.001	1.096	1.096	0.000
C_6-C_8	1.402	1.402	0.000	1.407	1.408	−0.001
C_8-H_9	1.071	1.073	−0.002	1.096	1.097	−0.001
C_8-C_{15}	1.398	1.398	0.000	1.406	1.406	0.000
			Interatomic Angles (deg)			
$X_1-N_2-C_3$	123.5	124.6	−1.1	123.5	123.9	−0.4
$C_{10}-N_2-C_3$	113.1	110.8	2.3	113.0	112.1	0.9
$N_2-C_3-C_5$	105.2	107.5	−2.3	105.0	106.1	−1.1
$O_4-C_3-C_5$	129.0	127.0	2.0	129.2	128.3	0.9
$C_3-C_5-C_6$	130.0	131.3	−1.3	129.9	130.6	−0.7
$C_{12}-C_5-C_6$	121.6	121.6	0.0	121.6	121.6	0.0
$C_5-C_6-C_8$	117.3	117.4	−0.1	117.3	117.3	0.0
$H_7-C_6-C_8$	121.5	121.6	−0.1	122.1	122.1	0.0
$C_6-C_8-C_{15}$	121.0	121.0	0.0	121.1	121.1	0.0
C_6-C8-H_9	119.6	119.6	0.0	119.6	119.7	−0.1

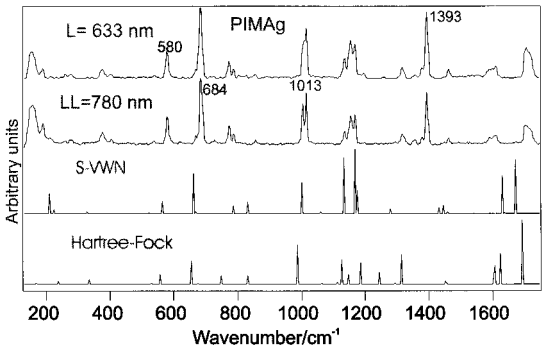

Figure 3. Raman spectrum of PIMAg salt recorded with the 633 nm laser line and the 780 nm laser lines. The bottom spectrum are the theoretical gas-phase Raman intensities calculated using S-VWN method.

between the gas-phase theoretical Raman spectra of the complex and the experimental spectrum is good. The Raman relative intensity pattern in this spectral region is successfully predicted by both theoretical computations. Next we consider the agreement in the upper part of the spectra. Here the two theoretical methods fail to predict the intensity of the 1393 cm^{-1} band. An immediate observation is that the gas-phase Hartree−Fock spectrum shows many more bands of substantial intensity than is observed in the PIMAg spectrum. The band at 1312 cm^{-1} is in the most obvious disagreement. Also, in the C═C and C═O region Hartree−Fock gives three bands with high intensity, where S-VWN gives two. The S-VWN spectrum is in better agreement with the observed PIMAg spectrum than Hartree−Fock, both in predicting the number of modes with high intensity and in the prediction of vibrational frequency. In summary, for the spectral region above 1000 cm^{-1}, the theoretical methods employed here fail to quantitatively reproduce the relative band intensities observed in the experimental SERS spectra. This shortcoming can be partly attributed to the basis set employed for these calculations. The basis set employed in this work, Lanl2DZ, is one of the only basis sets available for both organic and late transition metals, and is relatively small. Past experience

TABLE 2: Observed and Calculated Raman Wavenumbers and Raman Intensities (in Å^4 amu^{-1}) of PIMAg S-VWN/ Lanl2DZ Level of Theory

mode	sym	wave number	scaled	Raman	observed	assignment
5	a_1	212	208	19.2	192	N−Ag stretching
8	a_1	334	328	1.2	377	CO bending
12	a_1	570	560	11.7	580	CC def + CO bend
14	a_1	670	658	37.3	684	CN bend + CC def
18	a_1	798	785	6.4	774	ring deformation
24	a_1	1019	1002	29.0	1013	CH bending
27	a_1	1151	1132	51.4	1153	CH bend + breathing
28	a_1	1185	1166	69.3	1166	CH bending
31	a_1	1300	1279	3.8	1314	CH bend + CN stret
32	a_1	1451	1427	4.7	1393	CC stretching
34	a_1	1478	1454	1.1	1462	CC stretching
35	a_1	1655	1627	19.6	1611	CC stretching
38	a_1	1702	1674	50.3	1706	CO stretching
40	a_1	3151	3098	86.6	3060	CH stretching
42	a_1	3172	3119	269.6	3084	CH stretching
3	a_2	139	137	1.6		CC torsion
10	a_2	459	451	0.6		CC torsion
13	a_2	669	658	0.5		CC torsion
17	a_2	796	782	0.0		CH wag + CC tors
21	a_2	910	895	0.1		CH wagging
23	a_2	1012	995	0.0		CH wagging
2	b_1	66	65	1.8		N−Ag wagging
4	b_1	171	169	0.3	192	CO wagging
6	b_1	229	225	3.1	263	CNC wagging
9	b_1	413	406	0.6	405	Ring torsion
16	b_1	718	706	0.6	726	CN+CH wagging
19	b_1	799	786	0.1	789	CN+CH wagging
22	b_1	978	962	0.0	952	CH wagging
1	b_2	42	41	0.5		N−Ag bending
7	b_2	230	226	3.1	218	N−Ag stretching
11	b_2	531	522	0.4	539	CO bending
15	b_2	678	667	1.5	669	CN bend + CC def
20	b_2	844	830	10.8	857	CC deformation
25	b_2	1076	1058	1.4	1005	CH bending
26	b_2	1138	1119	0.0	1135	CH bend + breathing
29	b_2	1195	1175	21.7	1166	CH bending
30	b_2	1276	1255	0.0	1195	CH bend + CN stret
33	b_2	1464	1440	7.7	1461	CC stretching
36	b_2	1656	1628	35.3	1591	CC stretching
37	b_2	1664	1636	0.5	1718	CO stretching
39	b_2	3139	3087	37.2		CH stretching
41	b_2	3161	3108	44.0	3073	CH stretching

computing vibrational properties of molecules has indicated that the calculation of spectral intensities requires much larger basis sets than is required to obtain acceptable harmonic frequencies, which can be easily scaled to compare with experimental fundamentals. Recent work by Halls and Schlegel[19] has shown that the dominant consideration in achieving quantitative Raman intensities in the double harmonic approximation is the quality of basis set employed. They found that, in comparison to infrared intensities, Raman intensities are extremely slow to converge and require extensive basis sets, augmented with additional polarization and diffuse functions. Therefore, a substantial contribution to the relative intensity differences between the simulated and experimental SERS spectra can be attributed to basis set effects. Observed Raman wavenumbers and the calculated spectra are listed in Table 2.

Interpretation of the Experimental SERS Spectra. The SERS spectra of phthalimide chemisorbed onto rough silver surfaces were recorded with three laser lines: 514.5, 633, and 780 nm. Silver colloids were prepared following the same procedures reported in the first study of PIMH.[13] SERS spectra obtained on silver islands films and colloids are presented in Figure 4. The top spectrum is one of many similar SERS spectra recorded using evaporated PIMH films. However, the SERS

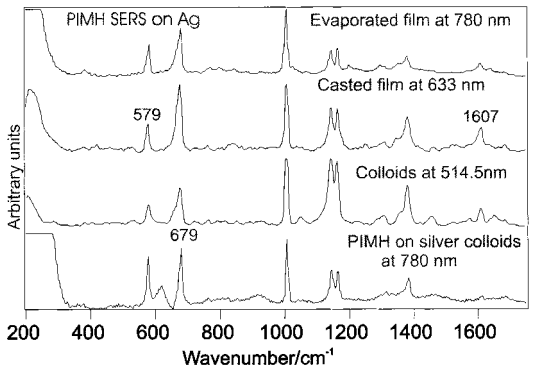

Figure 4. SERS spectra of PIMH on silver islands and colloidal silver.

spectra shown in Figure 4 do not agree with the reported SERS spectrum reported by Tsai and co-workers, obtained from a spin-coated thin solid film of PIMH on a silver island film using the 514.5 nm excitation (Figure 3, ref 14). The reproducibility of the results presented in Figure 4 was tested by fabricating several PIMH samples by vacuum evaporation with mass thickness between 10 and 30 nm onto silver island films. In all the experiments, reproducible SERS spectra were obtained. However, the effect of increased laser power is evident under the optical microscope where changes in the color of the film exposed to laser power higher than 1 mW can be seen. The latter indicates the surface complex is light sensitive and that photochemistry or photodissociation is occurring. The same SERS spectrum is obtained when a phthalimide film is casted onto the silver islands using phthalimide solution in ethanol and acetone. The SERS spectrum obtained at 633 nm is shown in Figure 4. Here again, the low radiant flux is the necessary condition to obtain reproducible SERS spectra. "Burning" of the surface complex results in the appearance of variable Raman spectra that ultimately gives the typical spectrum of carbon on the surface. The SERS spectra of PIMH on silver colloids are shown for the two extreme laser line frequencies. The SERS spectra are also practically the same spectra observed on island films. The advantage of colloidal SERS is that they are more resilient to the effect of the radiant flux. In summary, the same SERS spectrum is observed for all laser lines and different adsorption techniques. The most important finding is that the SERS spectra are in agreement with the Raman scattering spectrum of the PIMAg complex, as can be seen by comparing Figures 3 and 4. The differences in intensities should be attributed to the fact that the PIMAg salt spectrum corresponds to a random molecular orientation in the solid salt, while the SERS spectra are due to surface complex with a preferred molecular orientation at the silver surface. Therefore, SERS spectrum of the complex may deviate from the Raman spectrum of the PIMAg in the bulk. The spectral evidence is sufficient to conclude that the PIMH on silver islands and silver colloids forms a PIMAg surface complex. The observed SERS spectrum is the electromagnetically enhanced spectrum of the surface complex.

The general procedure for the interpretation of chemisorbed SERS spectra consists of the following basic steps: (1) identifying or choosing a molecular complex to model the surface species, (2) computing the normal modes, vibrational frequencies and polarizability derivative tensor elements, and (3) assuming an orientation of the complex that will allow the computation of simulated SERS spectra using only the relevant polarizability derivative tensor elements for each irreducible representation (by virtue of their alignment with the electric field at the surface).

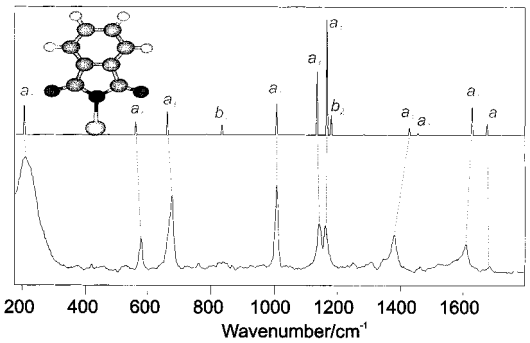

Figure 5. Correlation of the simulated S-VWN SERS spectrum and the experimental SERS spectrum showing symmetry assignments.

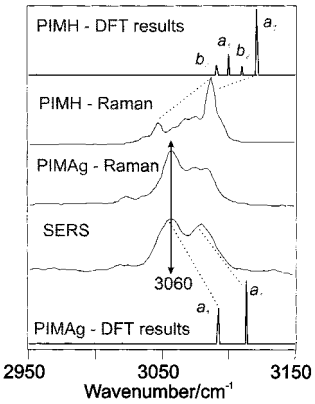

Figure 6. Calculated and observed Raman spectra of the C−H stretching modes of the PIMH, the PIMAg and the oriented surface complex.

The constraint in the free-molecule selection rules due to molecular orientation at the surface interface and the variation of the tangential and normal components of the electric field components at the surface determine the SERS selection rules.[34,35] Assuming a predominant normal component, it is expected then that the normal modes with polarizability derivative components perpendicular to the surface should dominate the SERS spectrum. With this assumption, the tangential electric field components are neglected in the following discussion. The molecular complex PIMAg is of C_{2v} symmetry and the molecular axes are such that that *z* contains the C_2 axis of symmetry and *yz* is the molecular plane. The electric field normal to the surface is assumed to be coincident with the C_2 axis along the N−Ag bond. Therefore, the strongest bands in the SERS spectrum should belong to normal modes transforming as **zz**. The next intense bands should belong to modes transforming as **xz** and **yz**. Finally, modes transforming as **xx**, **xy**, and **yy** should have very weak intensity and may not be observed at all. Applying this treatment to the theoretical PIMH SERS spectrum, the modes of irreducible representation a_1 should be most intense transforming as **xx, yy**, and **zz**. Modes of irreducible representation b_1 and b_2, transforming as **xz** and **yz**, respectively, may also be observed. Finally, vibrational modes of irreducible representation a_2, transforming as **xy**, should not be apparent since they have no *z* polarizability derivative component. In the double harmonic approximation, the Raman intensity is proportional to the polarizability derivative with respect to the normal coordinate squared ($I_{\text{Raman}} \propto |\partial\alpha_{ij}/\partial Q_k|^2$). The gas-phase theoretical Raman spectra can be made more comparable to the experimental SERS spectrum by computing the relative band intensities from the square of the **iz** ($i = x, y$, and *z*) polarizability derivative tensor elements computed with respect to normal coordinate displacements, which is readily obtained from quantum chemistry packages such as Gaussian98. This procedure discards modes of a_2 symmetry.

To obtain acceptable harmonic frequencies, which can be easily scaled to compare with experimental fundamentals, a much smaller basis set is required than is needed to predict vibrational band intensities. The basis set employed in this work, Lanl2DZ, is one of the only reliable basis sets for both organic and late transition metals and is relatively small.

The final correlation between the S-VWN simulated SERS spectrum using the model presented here and experimental SERS spectrum, along with symmetry assignments, is shown in Figure 5. Assignments were based on visualization of normal-mode displacement vectors and on frequency agreement. In this study, the S-VWN scaled harmonics were found to be in similar agreement with experimental SERS frequencies as was observed by Wong in comparing S-VWN computed harmonics and experimental gas-phase fundamentals for 122 molecules. The average difference between S-VWN scaled harmonic frequencies and observed SERS frequencies was 31 cm^{-1}. It can be seen that the experimental SERS spectrum is dominated by modes of a_1 symmetry, as is expected from the constraint of surface selection rules.

The characteristic C−H stretching modes give further support to the interpretation of the SERS spectrum presented above. In the Raman spectrum of the PIMH both the a_1 and the b_2 modes are observed in agreement with the computed spectrum as shown in Figure 6. However, a different pattern is observed in the Raman spectrum of the PIMAg complex, where only two a_1 modes (3084 and 3060 cm^{-1}) and one b_2 mode at 3073 cm^{-1} are observed. The predicted spectrum for the surface complex with a head-on molecular orientation contains solely the two a_1 modes in full agreement with the observed SERS spectra shown in Figure 6. The calculated harmonic C−H wavenumbers shown in Figure 6 are higher than the observed C−H stretching vibrations due to a sizable value of the anharmonicity in C−H stretching modes.

Conclusions

The Raman spectrum of the phthalimide−Ag salt was found to be in agreement with the observed SERS spectra of phthalimide adsorbed onto silver films and silver colloids. The SERS spectrum is conserved, independent of the origin of the phthalimide state: vacuum evaporated onto Ag, PIMH dissolved in organic solvents or from aqueous solutions of the PIMK salt. It is concluded that the origin of the SERS spectrum is due to the formation of the PIMAg complex on silver surfaces. Since the same SERS spectrum was obtained with laser lines from 514.5 to 780 nm, it was concluded that there no evidence of new electronic states, at least in this spectral region, that could serve as intermediate in the observation of resonance Raman scattering. Therefore, the "chemical effect" is determined by the formation of the surface complex without the complication of resonance Raman due to new electronic states or charge transfer states. The interpretation of the SERS spectrum follows the common vibrational approach whereby the symmetry species for the complex are discussed, in conjunction with the constraints imposed by the field polarization at the surface and the molecular orientation of the complex (SERS selection rules). It was also shown that ab initio methods are effective in simulating surface-complex spectra providing valuable support to the interpretation of the observed SERS spectrum.

Acknowledgment. R.F.A. gratefully acknowledges financial support from the Natural Science and Engineering Research

Council of Canada (NSERC), and M.D.H. and H.B.S. acknowledge financial assistance from the National Science Foundation (Grant No. CHE9874005). M.D.H. also thanks the Graduate School and Chemistry Department for financial support provided by Thomas C. Rumble and Wilfred Heller Graduate Fellowships.

References and Notes

(1) Fleischman, M.; Hendra, P. J.; McQuillan, A. J. *Chem. Phys. Lett.* **1974**, *26*, 163.
(2) Jeanmaire, D. J.; Van Duyne, R. P. *J. Electroanal. Chem.* **1977**, *84*, 1.
(3) Albrecht, M. G.; Creighton, J. A. *J. Am. Chem. Soc.* **1977**, *99*, 5215.
(4) Hartstein, A.; Kirtley, J. R.; Tsang, J. C. *Phys. Rev. Lett.* **1980,** 45, 201
(5) Nie, S.; Emory, S. R. *Science* **275** 1997 1102.
(6) Kneipp, K.; Kneipp, H.; Kartha, V. B.; Manoharan, R.; Deinum, G.; Itzkan, I.; Dasari, R. R.; Feld, M. S. *Phys. Rev. E* **1998**, *57*, R6281.
(7) Otto, A. In *Light Scattering in Solids*; Cardona, M., Guentherodt, G., Eds.; Springer: Berlin, 1984.
(8) Moskovits, M. *Rev. Mod. Phys.* **1985**, *57*, 783.
(9) Kambhampati, P.; Child, C. M.; Foster, M. C.; Campion, A. *J. Chem. Phys.* **1998**, *108*, 5013.
(10) Hase, Y. *J. Mol. Struct.* **1978**, *48*, 33.
(11) Bigoto, A.; Galaso, V. *Spectrochim. Acta* **1979**, *35A*, 725.
(12) Arenas, J. F.; Marcos, J. I.; Ramirez, F. J. *Appl. Spectrosc.* **1989**, *43*, 118.
(13) Aroca, R.; Clavijo, R. E. *Spectrochim. Acta A* **1988**, *44*, 171.
(14) Tsai, W. H.; Young, J. T.; Boerio, F. J.; Hong, P. P. *Langmuir* **1991**, *7*, 745.
(15) Scott, A. P.; Radom, L. *J. Phys. Chem.* **1996**, *100*, 16502.
(16) Wong, M. W. *Chem. Phys. Lett.* **1996**, *256*, 391.
(17) For example, reported scaling factors for DFT methods with the 6-31G(d) basis set are 0.9833 for S-VWN and 0.9945 for B-LYP. By contrast, the scale factors for conventional methods are 0.8953, 0.9427 and 0.9537 for Hartree−Fock, MP2 and QCISD, respectively. (From refs 15 and 16)
(18) Halls, M. D.; Schlegel, H. B. *J. Chem. Phys.* **1998**, *109*, 10587.
(19) Halls, M. D.; Schlegel, H. B. *J. Chem. Phys.* **1999**, *111*, 8819.
(20) Yang, W. H.; Shatz, G. C. *J. Chem. Phys.* **1992**, *97*, 3831.
(21) Yang, W. H.; Hulteen, J.; Shatz, G. C.; Van Duyne, R. P. *J. Chem. Phys.* **1996**, *104*, 4313.
(22) *Gaussian 99*, Development Version (Revision A.8); M. J. Frisch, G. W. Trucks, H. B. Schlegel, G. E. Scuseria, M. A. Robb, J. R. Cheeseman, V. G. Zakrzewski, J. A. Montgomery, Jr., R. E. Stratmann, J. C. Burant, S. Dapprich, J. M. Millam, A. D. Daniels, K. N. Kudin, M. C. Strain, O. Farkas, J. Tomasi, V. Barone, M. Cossi, R. Cammi, B. Mennucci, C. Pomelli, C. Adamo, S. Clifford, J. Ochterski, G. A. Petersson, P. Y. Ayala, Q. Cui, K. Morokuma, D. K. Malick, A. D. Rabuck, K. Raghavachari, J. B. Foresman, J. V. Ortiz, A. G. Baboul, J. Cioslowski, B. B. Stefanov, G. Liu, A. Liashenko, P. Piskorz, I. Komaromi, R. Gomperts, R. L. Martin, D. J. Fox, T. Keith, M. A. Al-Laham, C. Y. Peng, A. Nanayakkara, C. Gonzalez, M. Challacombe, P. M. W. Gill, B. Johnson, W. Chen, M. W. Wong, J. L. Andres, C. Gonzalez, M. Head-Gordon, E. S. Replogle, and J. A. Pople, Gaussian, Inc.: Pittsburgh, PA, 1998.
(23) Dunning, T. H.; Hay, P. J. In *Methods of Electronic Structure Theory*; Schaefer, H. F., Ed.; Plenum Press: New York, 1977; Vol 2.
(24) Hay, P. J.; Wadt, W. R. *J. Chem. Phys.* **1985**, *82*, 299.
(25) Slater, J. C. In *Quantum Theory of Molecules and Solids*; . McGraw-Hill: New York, 1974; Vol. 4.
(26) Vosko, S. J.; Wilk, L.; Nusair, M. *Can. J. Phys.* **1980**, *58*, 1200.
(27) Zerbi, G. In *Vibrational Intensities in Infrared and Raman Spectroscopy*; Person, Zerbi, Eds.; Elsevier: New York, 1982.
(28) Pople, J. A.; Schlegel, H. B.; Krishnan, R.; Defrees, J. S.; Binkley, J. S.; Frisch, M. J.; Whiteside, R. A. *Int. J. Quantum Chem. Quantum Chem. Symp.* **1981**, *15*, 269.
(29) Pulay, P.; Fogarasi, G.; Pongor, G.; Boggs, J. E.; Vargha, A. *J. Am. Chem. Soc.* **1983**, *105*, 7037.
(30) Fogarasi, G.; Pulay, P. *J. Mol. Struct.* **1977**, *39*, 275.
(31) Botschwina, P.; Meyer, W.; Semkow, A. M. *Chem. Phys.* **1976**, *15*, 25.
(32) Panchenko, Y. N. *Russ. Chem. Bull.* **1996**, *45*, 753.
(33) Creighton, J. A. In *Advances in Spectroscopy, Vol. 16, Spectroscopy of Surfaces*; Clark, R. J. H., Hester, R. E.Eds.; Wiley: New York, 1988, and references therein.
(34) Moskovits, M. *J. Chem. Phys.* **1982**, *77*, 4408, and references therein.
(35) Moskovits, M.; Suh, J. S. *J. Phys. Chem.* **1984**, *88*, 5526.